Preservation of benthic foraminifera and reliability of deep-sea temperature records: Importance of sedimentation rates, lithology, and the need to examine test wall structure

Journal Item

Preservation of benthic foraminifera and reliability of deep-sea temperature records: Importance of sedimentation rates, lithology, and the need to examine test wall structure

Philip F. Sexton[1,2] and Paul A. Wilson[3]

Received 12 June 2008; revised 19 January 2009; accepted 5 February 2009; published 9 May 2009.

[1] Preservation of planktic foraminiferal calcite has received widespread attention in recent years, but the taphonomy of benthic foraminiferal calcite and its influence on the deep-sea palaeotemperature record have gone comparatively unreported. Numerical modeling indicates that the carbonate recrystallization histories of deep-sea sections are dominated by events in their early burial history, meaning that the degree of exchange between sediments and pore fluids during the early postburial phase holds the key to determining the palaeotemperature significance of diagenetic alteration of benthic foraminifera. Postburial sedimentation rate and lithology are likely to be important determinants of the paleoceanographic significance of this sediment–pore fluid interaction. Here we report an investigation of the impact of extreme change in sedimentation rate (a prolonged and widespread Upper Cretaceous hiatus in the North Atlantic Ocean) on the preservation and δ^{18}O of benthic foraminifera of Middle Cretaceous age (nannofossil zone NC10, uppermost Albian/lowermost Cenomanian, ~99 Ma ago) from multiple drill sites. At sites where this hiatus immediately overlies NC10, benthic foraminifera appear to display at least moderate preservation of the whole test. However, on closer inspection, these tests are shown to be extremely poorly preserved internally and yield δ^{18}O values substantially higher than those from contemporaneous better preserved benthic foraminifera at sites without an immediately overlying hiatus. These high δ^{18}O values are interpreted to indicate alteration close to the seafloor in cooler waters during the Late Cretaceous hiatus. Intersite differences in lithology modulate the diagenetic impact of this extreme change in sedimentation rate. Our results highlight the importance of thorough examination of benthic foraminiferal wall structures and lend support to the view that sedimentation rate and lithology are key factors controlling the paleoceanographic significance of diagenetic alteration of biogenic carbonates.

Citation: Sexton, P. F., and P. A. Wilson (2009), Preservation of benthic foraminifera and reliability of deep-sea temperature records: Importance of sedimentation rates, lithology, and the need to examine test wall structure, *Paleoceanography*, *24*, PA2208, doi:10.1029/2008PA001650.

1. Introduction

1.1. Foraminiferal Preservation: Planktics Versus Benthics

[2] The preservation of planktic foraminiferal calcite has received widespread attention in the past decade [*Schrag et al.*, 1995; *Wilson and Opdyke*, 1996; *Norris and Wilson*, 1998; *Crowley and Zachos*, 2000; *Wilson and Norris*, 2001; *Pearson et al.*, 2001; *Norris et al.*, 2002; *Wilson et al.*, 2002; *Zachos et al.*, 2002; *Sexton et al.*, 2006a, 2006b; *Moriya et al.*, 2007; *Pearson et al.*, 2007]. This attention is primarily a consequence of attempts to accurately reconstruct sea surface temperatures (SSTs), especially for past warm climates (e.g., the early through middle Eocene and mid-Cretaceous). Partly on the basis of oxygen isotope ratios (δ^{18}O) of planktic foraminiferal calcite, we know that these intervals of geologic time are characterized by high-latitude temperatures that are consistently much warmer than those seen today [*Stott et al.*, 1990; *Barrera and Huber*, 1991; *Zachos et al.*, 1994; *Huber et al.*, 1995]. Yet for many years, foraminiferal δ^{18}O-derived SST estimates from the contemporaneous tropical oceans were thought to have been no warmer or even cooler than the modern tropics [*Douglas and Savin*, 1973, 1975; *Savin*, 1977; *Shackleton and Boersma*, 1981; *Boersma et al.*, 1987; *Crowley*, 1991; *Barrera*, 1994; *Zachos et al.*, 1994; *Bralower et al.*, 1995; *Price et al.*, 1998]. These cool δ^{18}O-derived tropical SSTs were at odds with the warmer-than-modern tropical SSTs predicted in numerical modeling experiments [e.g., *Manabe and Bryan*, 1985; *Sloan and Rea*, 1996; *Bush and Philander*, 1997; *Huber and Sloan*, 2000, 2001; *Poulsen et al.*, 2001]. This so-called "Cool Tropic Paradox" [*D'Hondt and Arthur*, 1996] has subsequently been explained as an artifact of diagenetic alteration of planktic foraminiferal calcite near the seafloor at tropical sites (where the vertical temperature gradient in the ocean is strong)

[1]Scripps Institution of Oceanography, University of California, San Diego, La Jolla, California, USA.
[2]Now at School of Earth and Ocean Sciences, Cardiff University, Cardiff, UK.
[3]National Oceanography Centre, University of Southampton, Southampton, UK.

0883-8305/09/2008PA001650$12.00

yielding artificially cool δ^{18}O-derived SSTs [*Schrag et al.*, 1995; *Wilson and Opdyke*, 1996; *Norris and Wilson*, 1998; *Wilson and Norris*, 2001; *Pearson et al.*, 2001; *Wilson et al.*, 2002; *Sexton et al.*, 2006a].

[3] In comparison to planktics, preservation of benthic foraminifera has received little attention [see *Corliss and Honjo*, 1981; *Widmark and Malmgren*, 1988; *Murray*, 1989; *McCorkle et al.*, 1995; *Carman and Keigwin*, 2004]. This situation is probably traceable in part to (1) the greater robustness of more heavily calcified benthic tests in comparison to planktics and (2) the realization that diagenetic alteration of benthics will, except at high-latitude sites of deep convection, tend to proceed in waters closer in temperature and composition to the waters in which the tests were secreted than is the case for planktics. Numerical modeling indicates that the carbonate recrystallization histories of deep-sea sections are dominated by events in their early burial history [*Rudnicki et al.*, 2001]. First, in line with

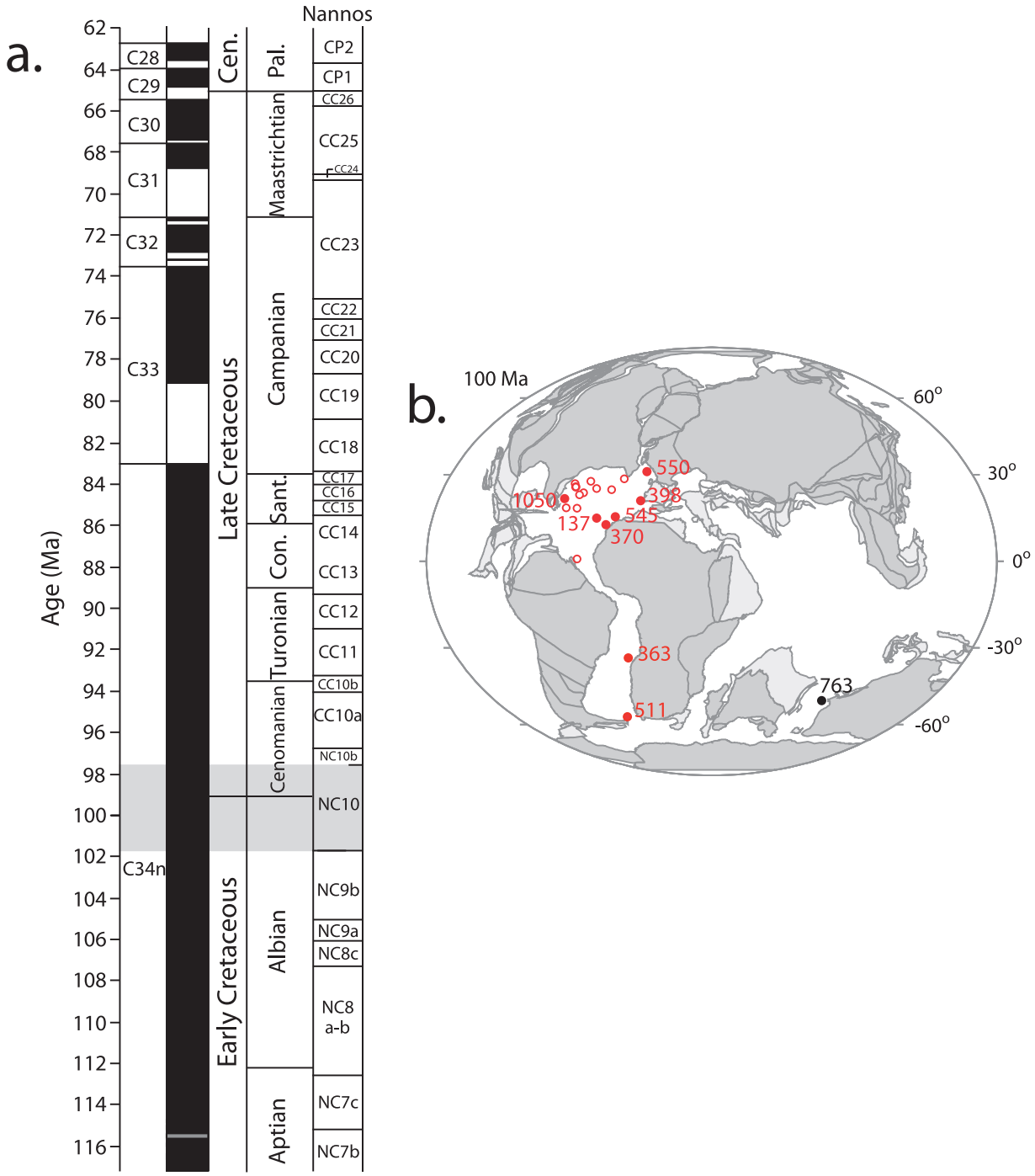

Figure 1

the view that clay-rich sediments enhance the preservation of planktic foraminifera [*Norris and Wilson*, 1998; *Wilson and Norris*, 2001; *Pearson et al.*, 2001; *Wilson et al.*, 2002; *Sexton et al.*, 2006a], lithological composition should also be an important factor governing the alteration of benthics. Second, postburial sedimentation rate, as well as being fundamental to controlling the impact of diagenetic alteration of bulk carbonate [*Schrag et al.*, 1995], will also likely be important to determining the palaeotemperature significance of alteration of benthic foraminifera. However, because numerical diagenetic models rely on pore fluid chemistry profiles that are controlled by the diagenesis of bulk carbonate (mainly calcareous nannofossils), these models cannot be used to evaluate the alteration pathway of the individually picked foraminifera that are used in palaeoceanographic studies. Here we investigate the impact of extreme change in sedimentation rate (a prolonged and widespread hiatus) and lithological variability on the preservation and $\delta^{18}O$ of benthic foraminifera of Middle Cretaceous age (nannofossil zone NC10, uppermost Albian/lowermost Cenomanian, ~99 Ma ago (Figure 1a)) from multiple drill sites in the North Atlantic Ocean.

1.2. Mid-Cretaceous

[4] The mid-Cretaceous represents an important interval in the evolution of Earth's climate. Diverse geological evidence indicates that, during this interval, Earth experienced some of the warmest temperatures of the entire Phanerozoic Era (last ~545 Ma) [*Crowley and North*, 1991; *Veizer et al.*, 2000]. This extreme warmth is widely interpreted to result from an increase in greenhouse forcing through elevated levels of atmospheric carbon dioxide [*Berner et al.*, 1983; *Barron and Washington*, 1985; *Schlanger et al.*, 1981; *Larson*, 1991; *Berner and Kothavala*, 2001; *Bice and Norris*, 2002]. Because of their relevance to climate scenarios for the coming centuries, it is important to understand the forcing mechanisms and dynamic feedbacks operating during these past warm climates. An essential prerequisite to developing this understanding is knowledge of the most basic regional and global features of this extreme warmth (and likewise, for patterns of carbon cycling). We are currently in the early stages of developing this observational database for mid-Cretaceous climates.

2. Materials and Methods

[5] Sediments were disaggregated by soaking in deionized water for 30 min and wet sieving through a 63 μm mesh. The coarse (>63 μm) fraction was dry sieved and benthic foraminifera were picked from the 212 to 350 μm size fraction. Monospecific specimens of either *Gyroidinoides infracretacea* or *Gavelinella* sp. were used for stable isotope analyses (paired analyses of these two species within the same sample yield minimal $\delta^{18}O$ offsets: *G. infracretacea* – *Gavelinella* sp. = 0.03‰ [1σ = 0.28‰, n = 33]). Oxygen isotope ratios were analyzed using a Europa Geo 20–20 mass spectrometer equipped with an automatic carbonate preparation system. Between 4 and 10 specimens were analyzed after ultrasonic cleaning in deionized water. $\delta^{18}O$ data are reported relative to the Vienna Peedee Belemnite standard (VPDB). Standard external analytical precision, based on replicate analyses of in-house standards calibrated to NBS-19, is ±0.08‰. Scanning electron micrographs were generated using a Leo 1450VP (variable pressure) digital Scanning Electron Microscope (SEM) fitted with a tungsten filament. Prior to SEM analysis, foraminiferal specimens were gold coated. Gold coating optimizes the backscattering of secondary electrons from the sample, providing better topographic imaging.

3. A Widespread Upper Cretaceous Hiatus in the North Atlantic

[6] A summary of results from the first decade and a half of deep-sea drilling revealed a widespread sedimentary hiatus through the Upper Cretaceous across the western part of the North Atlantic [*Arthur and Dean*, 1986]. This hiatus, with its base typically occurring in the lower Cenomanian, was observed at 11 of the 18 DSDP drill sites examined in this synthesis [*Arthur and Dean*, 1986] (Figure 1b). Here we extend these earlier observations by examining (1) additional old DSDP sites from the eastern half of the North Atlantic basin and (2) newer drill sites from more recent ocean drilling.

[7] Figure 1 shows the location of all DSDP and ODP drill sites studied here along with those shown to contain an Upper Cretaceous hiatus in the earlier synthesis (all sites with this hiatus are labeled in red). Figure 2 depicts our new evaluation of the timing, duration and stratigraphic position of the Upper Cretaceous hiatus at our studied sites. Figure 2 shows that the base of the hiatus (colored red) occurs at a broadly similar age across sites, toward the top of NC10 around 99 Ma ago, in the lowermost Cenomanian (biozone NC10 colored gray) (ages referred to here are based on updated calcareous microfossil biozonation chronologies [e.g., *Erba et al.*, 1995; *Bralower et al.*, 1997; *Burnett*,

Figure 1. (a) Magnetobiostratigraphic timescale for the Cretaceous epoch (modified from *Shipboard Scientific Party* [2004]). Gray shading shows the stratigraphic position of calcareous nannofossil biozone NC10, the target interval for this study. A new astrochronology dates the lower and upper boundaries of biozone NC10 at 100.95 and 99.55 Ma, respectively [*Watkins et al.*, 2005]. (b) Paleogeographic reconstruction for the Albian-Cenomanian boundary (biozone NC10, ~100 Ma; before equatorial Atlantic gateway opening) showing the location of DSDP and ODP drill sites discussed here. All red circles (solid and open) show sites with a hiatus through the Upper Cretaceous. Solid red circles denote DSDP/ODP sites (numbered on the map) studied here, whereas open red circles (not numbered to avoid clutter) denote those studied by *Arthur and Dean* [1986]. DSDP site numbers for the open red circles are 101, 105, 144, 384, 386, 387, 390, 391, 392, 417, and 534. Dark gray shading denotes emergent continental fragments. Light gray shading denotes submerged continental shelves. Paleogeographic map is from the Ocean Drilling Stratigraphic Network plate tectonic reconstruction service (http://www.odsn.de/odsn/services/paleomap/paleomap.html).

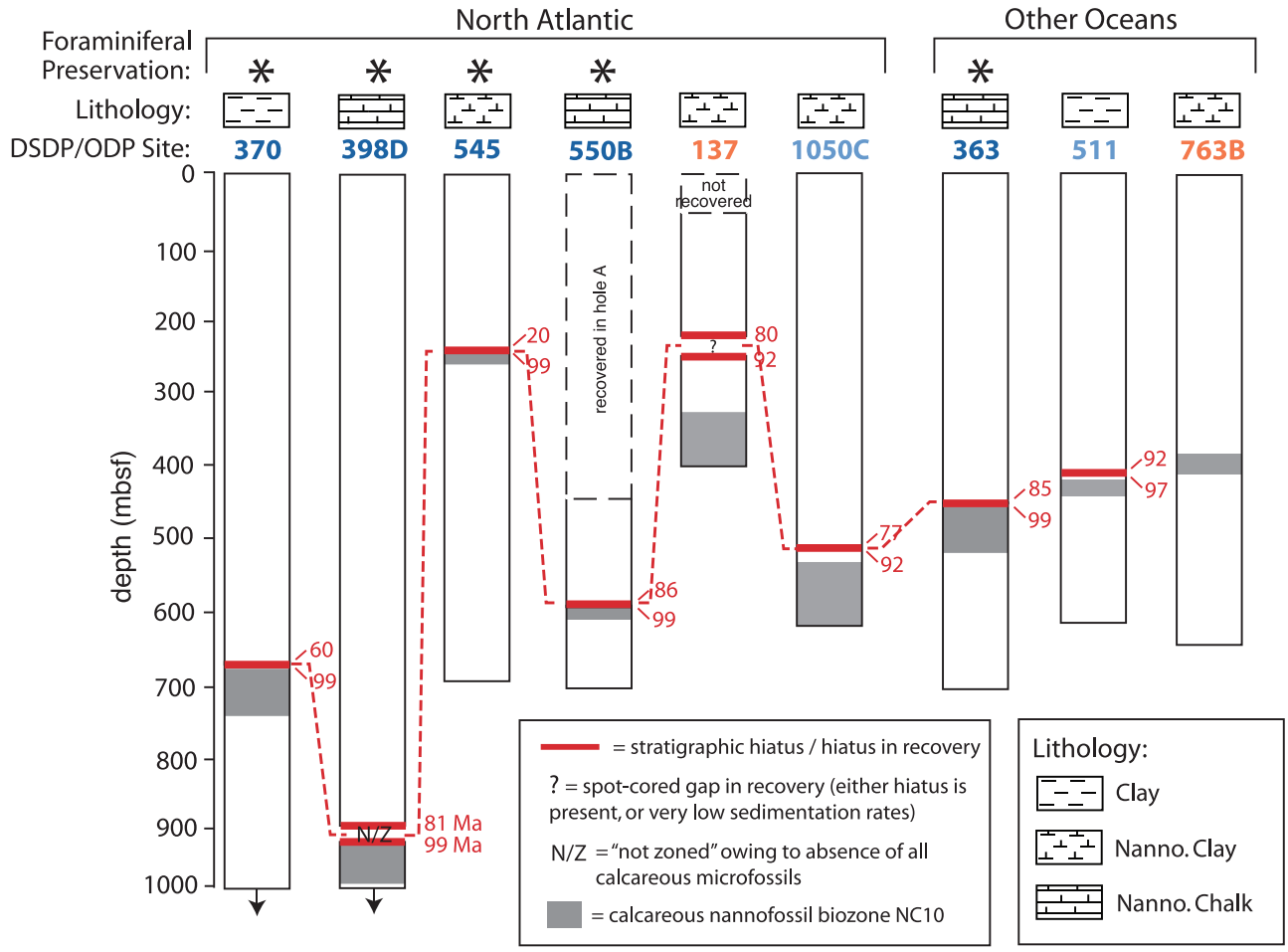

Figure 2. Timing, duration, and stratigraphic position of the Upper Cretaceous hiatus (marked by red horizontal lines) across multiple drill sites. Gray shaded areas define the stratigraphic range of calcareous nannofossil biozone NC10 at each site. Colors of the DSDP/ODP site numbers refer to the stratigraphic position of the hiatus with respect to NC10 (dark blue, a hiatus immediately overlying NC10; light blue, a hiatus just above NC10; orange, no hiatus or its base occurs further up section). Red numbers indicate the ages (in millions of years ago) of the top and the base of the hiatus at each site. Sites that host severely diagenetically altered NC10 benthic foraminifera (see Figure 3) are marked by asterisks. Note that the sites with a hiatus immediately overlying biozone NC10 (dark blue site numbers) also host diagenetically altered NC10 foraminifera. Biostratigraphies for each site are from *Bice et al.* [2003], *Hayes et al.* [1972], *Shipboard Scientific Party and Bukry* [1978], and *Shipboard Scientific Party* [1978, 1979, 1983, 1984, 1985, 1990, 1998].

1999; *Premoli Silva and Sliter*, 1999; *Watkins et al.*, 2005]). At DSDP Site 137 and ODP Site 1050, the base of the hiatus occurs significantly later (at 92 Ma ago) than at the other sites. The age for the top of the hiatus is more variable, generally falling anywhere from 88 to 77 Ma ago (Coniacian to middle Campanian), meaning that the duration of the hiatus is typically between 11 and 22 Ma ago (notwithstanding its anomalously long duration at Site 545). At Site 137 the hiatus, or at least an extremely condensed horizon, is inferred to occur on the basis of large differences in the age of sediments either side of a short core gap. At Site 398D, the same time interval represented by a hiatus at other sites is here characterized by a transition from carbonate-bearing sediment to carbonate-free clay with very low sedimentation rates. All DSDP and ODP drill sites exhibiting an Upper Cretaceous hiatus are situated in the North

Figure 3. Scanning electron micrographs of benthic foraminifera whole tests and wall cross sections from mid-Cretaceous calcareous nannofossil biozone NC10. Numbers refer to DSDP and ODP sites. Sites that host severely diagenetically altered foraminifera (restricted to the North Atlantic, apart from Site 363) are marked by asterisks. The scale bar for whole tests is 100 μm; the scale bar for wall cross sections is 10 μm.

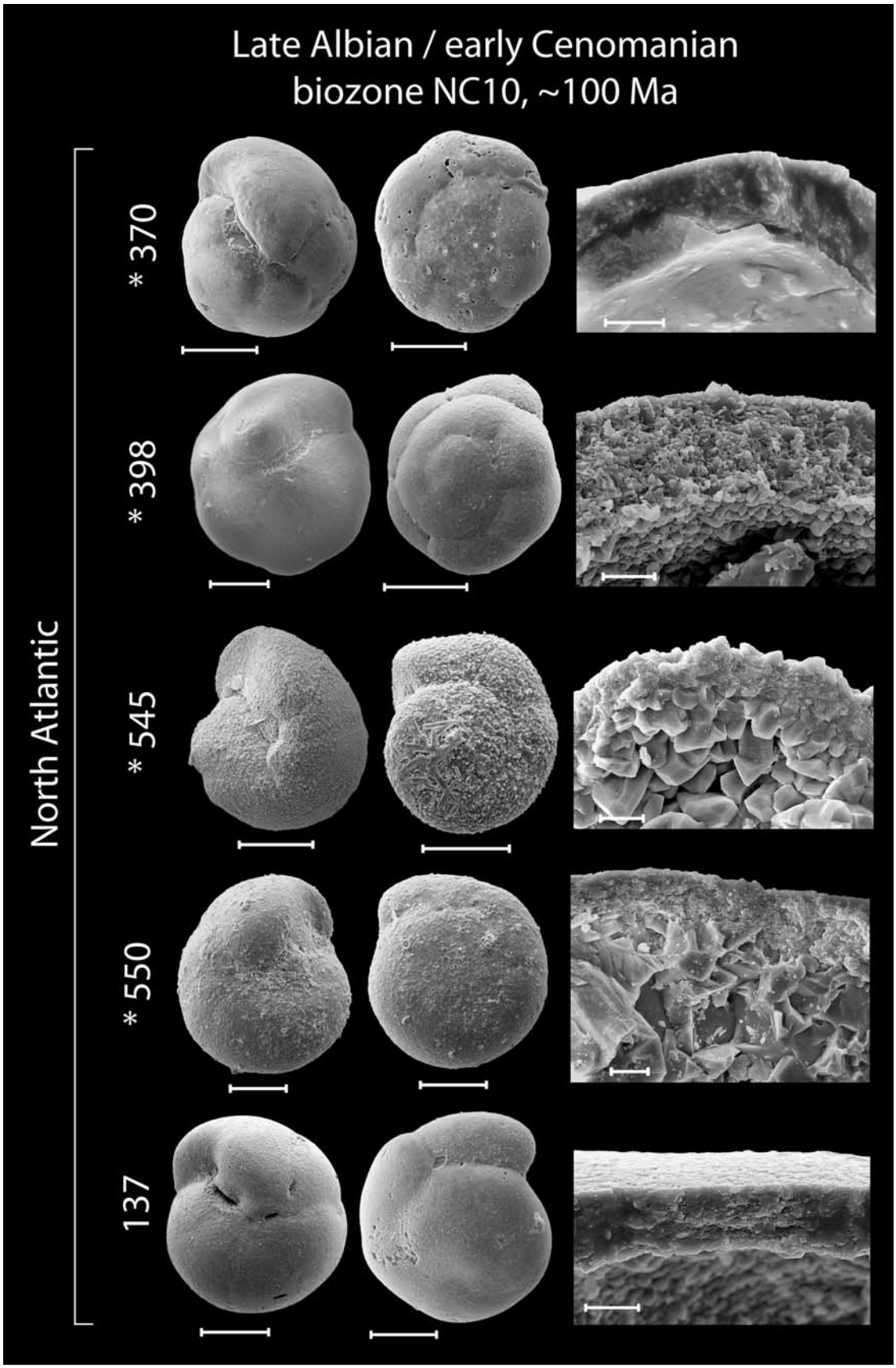
Late Albian / early Cenomanian
biozone NC10, ~100 Ma
North Atlantic
* 370
* 398
* 545
* 550
137

Figure 3

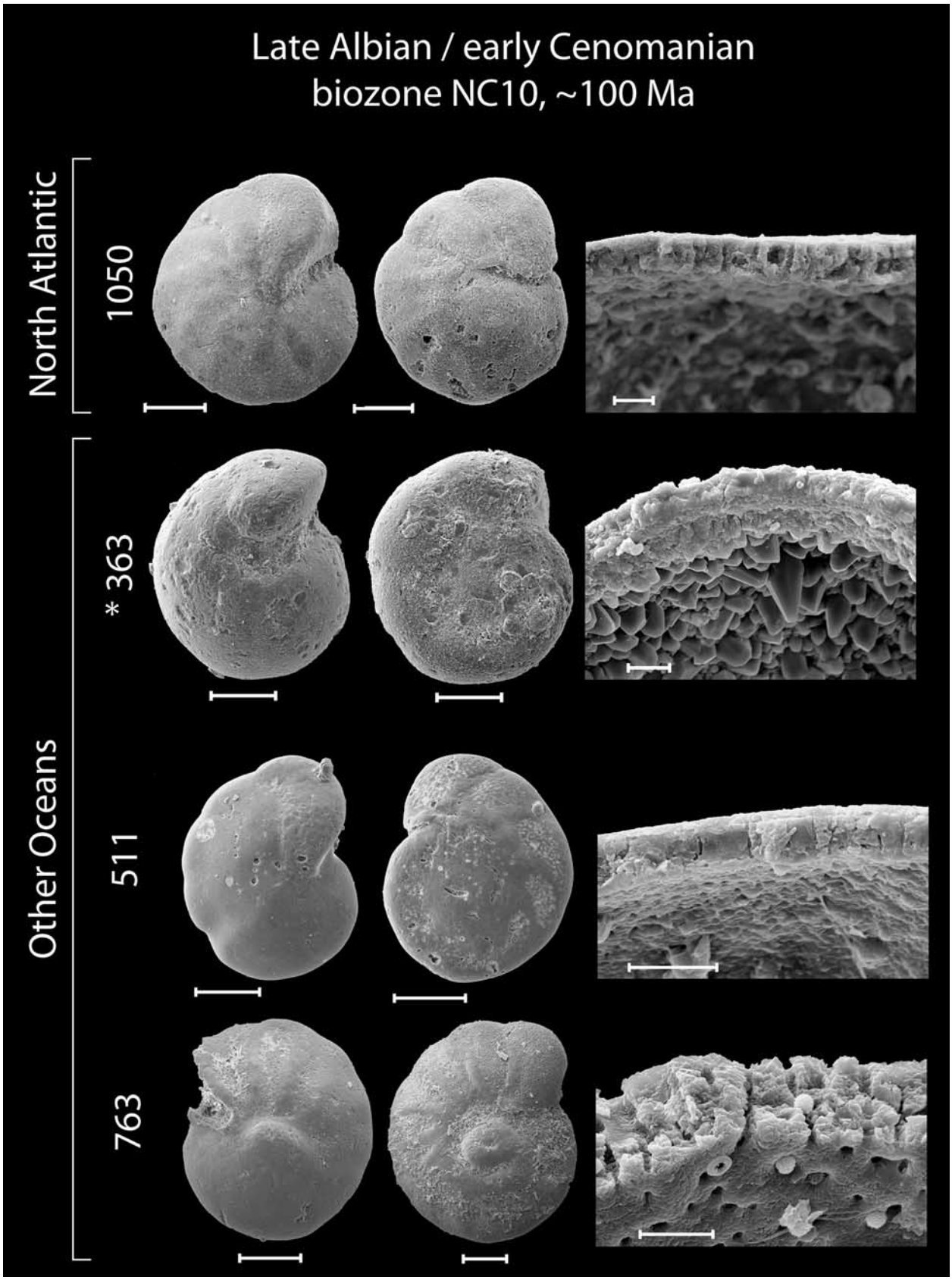

Figure 3. (continued)

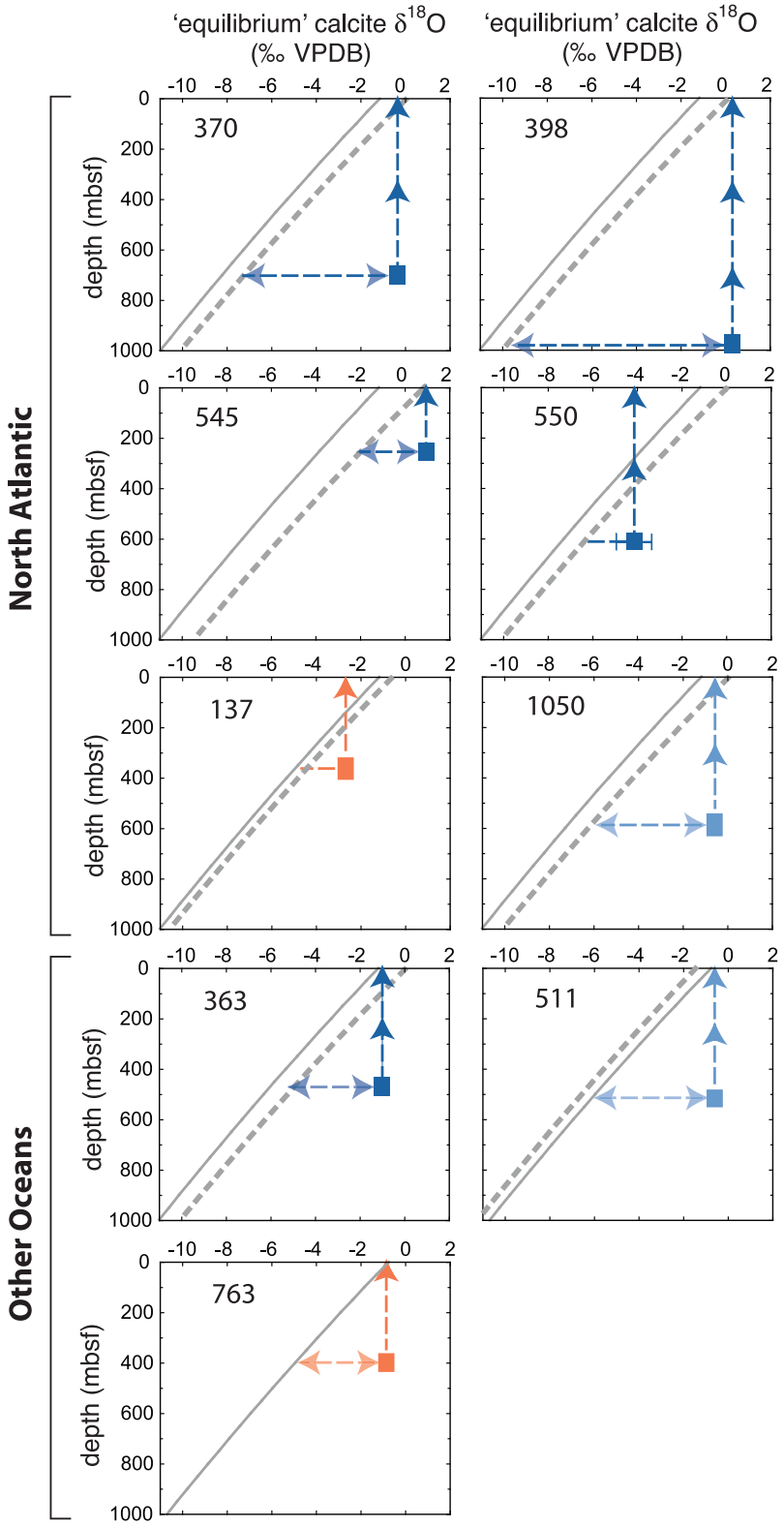
'equilibrium' calcite δ18O (‰ VPDB)
'equilibrium' calcite δ18O (‰ VPDB)
North Atlantic
Other Oceans
depth (mbsf)
370
398
545
550
137
1050
363
511
763

Figure 4

Atlantic except for DSDP Site 363 in the northern South Atlantic and Site 511 (with an unusually short hiatus) in the southern South Atlantic (Figures 1b and 2). The hiatus is absent from Site 763B in the Indian Ocean (Figure 2).

4. Taphonomy: Relationship to Sedimentation Rate and Lithology

[8] Figure 3 shows scanning electron micrographs of representative benthic foraminifera from biozone NC10 for each of the drill sites studied. We show images of whole tests and higher-magnification views of test wall cross sections and chamber interiors. Images of whole tests appear to indicate at least moderate preservation of foraminifera at all sites. However, test wall cross sections and chamber interior views reveal a very different picture: benthic foraminifera from those sites with a hiatus immediately overlying the host NC10 strata (site numbers colored dark blue in Figure 2) are extremely poorly preserved (marked by asterisks in Figure 3). These images reveal abundant, large crystals of inorganic calcite growing on interior walls (Sites 398, 545, 550 and 363) and an apparently less severely altered, "melted" fabric in wall cross section (Site 370) suggestive of neomorphic alteration [e.g., *Sexton et al.*, 2006a]. Other drill sites where the hiatus falls slightly further up section (Sites 1050C and 511) (site numbers colored light blue in Figure 2) yield foraminifera with a range of taphonomies. Sites where the hiatus falls much further up section (Site 137) or not at all (Site 763B) (site numbers colored orange in Figure 2) show noticeably better preserved benthic foraminifera from calcareous nannofossil biozone NC10 (Figure 3), suggesting a link between the hiatus and severe diagenetic alteration of calcareous microfossils in immediately underlying sediments.

5. Impact of Diagenetic Alteration on Benthic Foraminiferal $\delta^{18}O$ Across the North Atlantic

[9] In Figure 4 we compare measured $\delta^{18}O$ for benthic foraminifera at all sites (data in Table 1) to the estimated value of $\delta^{18}O$ of calcite grown in isotopic equilibrium with pore waters at these sites across a range of depths from the seafloor to 1000 m burial for two time slices: (1) the interval during which the foraminifera lived (biozone NC10, solid gray line) and (2) the interval of the hiatus (dashed gray line). We estimate $\delta^{18}O$ of "equilibrium calcite" using a gradient in $\delta^{18}O$ of pore fluid of -2.5‰/km [*Lawrence and Gieskes*, 1981], a conservative geothermal temperature gradient of 40°C/km [*Rao et al.*, 2001] and local bottom water temperatures (BWTs) for the two time slices taken from *Poulsen et al.* [2001] and *Huber et al.* [2002]. Thus, the offset in the two equilibrium calcite lines simply reflects Cretaceous long-term cooling of deep-sea temperatures from NC10 to the time frame represented by the hiatus. We plot average $\delta^{18}O$ values for multiple analyses of benthic foraminifera at each site (see Table 1) against present burial depth (dark blue = sites with a hiatus immediately overlying NC10; light blue = sites with a hiatus just above NC10; orange = sites without a hiatus, or hiatus occurs much further up section). The distance along the horizontal axes between the intersection points of the vertical colored dashed lines and the solid gray lines with the seafloor (0 m below seafloor (mbsf)) represents the offset between measured and estimated equilibrium foraminiferal calcite $\delta^{18}O$ for NC10. Thus, the greater this distance, the more diagentically altered we interpret the measured $\delta^{18}O$ value to be. Foraminifera from sites outside the North Atlantic (Sites 363, 511, 763) yield $\delta^{18}O$ values that are similar to both one another and to equilibrium calcite at the seafloor during NC10. Of the North Atlantic sites, those where the base of the hiatus occurs well above NC10 (orange symbols) host benthic foraminifera with $\delta^{18}O$ values that are lower than those for equilibrium calcite at the seafloor during NC10 (Site 137), indicative of warmer paleotemperatures than the model-derived estimates [*Poulsen et al.*, 2001] used in calculating equilibrium $\delta^{18}O$. However, North Atlantic sites where the base of the Upper Cretaceous hiatus immediately overlies NC10 (dark blue) host benthic foraminifera with $\delta^{18}O$ values that are generally significantly higher than those for equilibrium calcite at the contemporaneous seafloor. The exception to this pattern is DSDP Site 550, where NC10 benthic foraminifera register much lower $\delta^{18}O$ values than any other site, and than equilibrium calcite at the seafloor. Finally, North Atlantic sites where the hiatus falls a little above NC10 (e.g., 1050) give intermediate paleotemperatures.

Figure 4. Average values for multiple $\delta^{18}O$ analyses of benthic foraminifera within NC10 (~99 Ma) at each site (colored squares) compared to estimated $\delta^{18}O$ of calcite grown in equilibrium with pore waters at these sites during two time slices: (1) NC10 (solid gray lines) and (2) the interval of the hiatus (dashed gray lines). Dark blue, hiatus immediately overlying NC10; light blue, hiatus just above NC10; orange, no hiatus or its base is further up section. Error bars denote 1σ of all $\delta^{18}O$ analyses within NC10 at each site. The absence of an error bar indicates 1σ error is less than the thickness of the symbol. Length of symbols along the y axis is proportional to the respective stratigraphic length of biozone NC10. The $\delta^{18}O$ of equilibrium calcite is estimated using a gradient in $\delta^{18}O$ of pore fluid of -2.5‰/km [*Lawrence and Gieskes*, 1981], a conservative geothermal temperature gradient of 40°C/km [*Rao et al.*, 2001], and "local" bottom water temperatures (BWTs) for the two time slices taken from *Poulsen et al.* [2001] and *Huber et al.* [2002]. BWTs used for NC10 are 16°C (North Atlantic sites) and 14°C (Sites 511 and 763). BWTs used for the interval of the hiatus are taken from the age of the top of the hiatus (or, where an interval of extremely low sedimentation rate must be inferred (see Figure 2), from the age of the hiatus' midpoint). Note that NC10 foraminifera from dark blue sites generally yield higher $\delta^{18}O$ than either light blue or orange sites and than $\delta^{18}O$ of equilibrium calcite at the seafloor (0 mbsf) during NC10 (solid lines). But NC10 foraminifera immediately underlying a hiatus (dark blue) generally yield very similar $\delta^{18}O$ to that of equilibrium calcite at the seafloor during the hiatus (dashed lines). Numbers refer to DSDP and ODP sites.

Table 1. List of all Stable Isotope Data Used in Figure 4 Along With Data Sources

Site	Core	Section	Top	Base	Depth (mbsf)	$\delta^{13}C$	$\delta^{18}O$	Species	Reference[a]
370	21	1	39.5	41.5	682.9	−1.062	0.006	*Gyroidinoides* sp.	1
370	23	1	99.5	102.5	702.49	−5.421	−1.179	*Gyroidinoides* sp.	1
370	23	3	100	103	705.5	−1.628	−0.205	*Gyroidinoides* sp.	1
370	24	2	93	96	713.43	−3.611	−1.243	*Gyroidinoides* sp.	1
370	24	4	60	63	716.1	−0.504	−0.898	*Gyroidinoides* sp.	1
398D	59	1	117	120	975.17	0.172	0.411	*Gyroidinoides infracretacea*	1
398D	59	2	40	43	975.9	0.782	0.081	*Gyroidinoides infracretacea*	1
398D	59	2	80	83	976.3	0.798	−0.289	*Gyroidinoides infracretacea*	1
398D	59	3	33	36	977.33	0.764	1.124	*Gyroidinoides infracretacea*	1
398D	60	2	40.5	43.5	985.41	0.495	1.008	*Gyroidinoides infracretacea*	1
398D	60	2	78.5	81.5	985.78	0.620	0.453	*Gyroidinoides infracretacea*	1
398D	59	2	40	43	975.9	1.014	0.269	*Gyroidinoides infracretacea*	1
398D	59	2	80	83	976.3	1.082	0.229	*Gyroidinoides infracretacea*	1
398D	59	3	33	36	977.33	0.857	0.993	*Gyroidinoides infracretacea*	1
398D	60	2	40.5	43.5	985.41	0.686	1.461	*Gyroidinoides infracretacea*	1
398D	60	2	78.5	81.5	985.78	0.512	−0.285	*Gyroidinoides infracretacea*	1
545	28	1	32	35.5	255.82	0.276	0.130	*Gyroidinoides infracretacea*	1
545	28	CC	4	7	256.36	0.455	0.619	*Gyroidinoides infracretacea*	1
545	29	2	14	17	266.35	0.510	1.415	*Gyroidinoides infracretacea*	1
545	29	2	40	44	266.61	0.248	0.559	*Gyroidinoides infracretacea*	1
545	30	1	40.5	43	274.9	−0.057	−0.120	*Gyroidinoides infracretacea*	1
550B	18	3	59	62	620.59	2.510	−2.378	*Gyroidinoides infracretacea*	1
550B	20	2	44	47	636.94	1.017	−6.116	*Gyroidinoides infracretacea*	1
137	13	3	46	48	323.46	0.196	−1.645	*Gyroidinoides infracretacea*	1
137	13	3	46	48	323.46	0.554	−1.94	*Gavelinella* sp.	1
137	13	3	91	93	323.91	0.437	−1.484	*Gyroidinoides infracretacea*	1
137	13	3	91	93	323.91	0.527	−1.876	*Gavelinella* sp.	1
137	14	1	107	109	340.07	0.142	−2.791	*Gyroidinoides infracretacea*	1
137	14	2	137	139	341.87	−0.182	−2.251	*Gyroidinoides infracretacea*	1
137	14	3	23	25	342.23	0.079	−2.781	*Gyroidinoides infracretacea*	1
137	14	3	76	78	342.76	0.196	−3.374	*Gyroidinoides infracretacea*	1
137	14	4	96	98	344.46	0.399	−2.607	*Gyroidinoides infracretacea*	1
137	14	4	96	98	344.46	0.764	−3.135	*Gavelinella* sp.	1
137	14	4	113	116	344.63	0.28	−1.996	*Gyroidinoides infracretacea*	1
137	14	4	113	116	344.63	0.849	−2.348	*Gavelinella* sp.	1
137	14	4	142	145	344.92	0.532	−2.1	*Gyroidinoides infracretacea*	1
137	14	5	12	14	345.12	0.341	−2.109	*Gyroidinoides infracretacea*	1
137	14	5	12	14	345.12	0.659	−2.532	*Gavelinella* sp.	1
137	14	5	24	26	345.24	0.156	−2.097	*Gyroidinoides infracretacea*	1
137	14	5	24	26	345.24	0.608	−2.399	*Gavelinella* sp.	1
137	14	5	57	59	345.57	0.113	−3.362	*Gyroidinoides infracretacea*	1
137	14	5	79	81	345.79	0.363	−2.531	*Gavelinella* sp.	1
137	14	5	96	98	345.96	0.349	−2.535	*Gyroidinoides infracretacea*	1
137	14	6	20	22	346.7	0.306	−2.764	*Gyroidinoides infracretacea*	1
137	15	2	36	38	349.86	0.624	−3.664	*Gyroidinoides infracretacea*	1
137	15	2	36	38	349.86	0.798	−2.773	*Gavelinella* sp.	1
137	15	2	116	118	350.66	−0.04	−2.841	*Gyroidinoides infracretacea*	1
137	16	3	43	45	378.43	0.856	−3.035	*Gavelinella* sp.	1
137	16	4	52	54	380.02	0.703	−3.416	*Gavelinella* sp.	1
1050	25	3	60	64	542.3	0.861	−0.705	*Berthelina* sp.	2
1050	25	4	16	20	543.36	1.501	−0.749	mixed benthics	2
1050	26	1	139	141	549.69	1.45	−0.722	*Gavelinella* sp.	2
1050	26	1	53	56	548.93	0.675	−0.646	*Gavelinella* sp.	2
1050	26	1	53	56	548.93	0.194	−0.717	*Berthelina* sp.	2
1050	26	2	56	59	550.46	1.035	−0.549	*Nuttalides* sp.	2
1050	26	3	120	122	552.6	0.077	−0.507	*Berthelina* spp.	2
1050	26	3	73	76	552.13	0.889	−0.586	*Berthelina* sp.	2
1050	26	4	140	142	554.3	−0.101	−0.903	*Berthelina* spp.	2
1050	26	4	83	86	553.73	0.504	−0.506	*Berthelina* spp.	2
1050	26	4	83	86	553.73	0.657	−0.619	*Gyroidina globosa*	2
1050	26	5	83	86	555.23	0.904	−0.837	*Berthelina* sp.	2
1050	26	CC	9	10	555.57	0.991	−0.538	*Gavelinella* sp.	2
1050	27	1	73	76	558.73	0.291	−0.768	*Gavelinella* sp.	2
1050	27	2	85	88	560.35	0.024	−0.924	*Berthelina* sp.	2
1050	27	2	85	88	560.35	0.688	−0.697	*Berthelina* spp.	2
1050	27	3	79	82	561.79	−0.012	−0.852	*Berthelina* sp.	2
1050	27	3	79	82	561.79	0.291	−0.297	*Berthelina* sp.	2
1050	27	4	134	136	563.84	0.42	0.15	*Berthelina* spp.	2
1050	27	4	34	36	562.84	−0.196	−0.81	*Berthelina* spp.	2
1050	27	4	80	83	563.3	0.468	−0.727	*Planulina* sp.	2
1050	27	5	123	125	565.23	0.728	−0.214	*Berthelina* spp.	2

Table 1. (continued)

Site	Core	Section	Top	Base	Depth (mbsf)	$\delta^{13}C$	$\delta^{18}O$	Species	Reference[a]
1050	27	5	32	34	564.32	0.111	−0.528	*Berthelina* sp.	2
1050	27	6	74	78	566.24	0.061	−0.597	*Berthelina* sp.	2
1050	27	6	74	78	566.24	0.137	−0.621	*Berthelina* sp.	2
1050	28	1	70	73	568.3	0.26	0.142	*Berthelina* sp.	2
1050	28	2	61	64	569.71	0.42	−0.626	*Berthelina* sp.	2
1050	28	3	60	63	571.2	−0.32	−0.946	*Berthelina* sp.	2
1050	28	4	146	150	573.56	−0.279	−0.813	*Berthelina* sp.	2
1050	28	4	66	69	572.76	0.422	−0.717	*Planulina* sp.	2
1050	28	5	50	53	574.1	0.018	−0.707	*Berthelina* sp.	2
1050	28	5	50	53	574.1	0.472	−0.639	*Berthelina* flat	2
1050	29	1	57	60	577.77	0.017	−0.49	*Berthelina* sp.	2
1050	29	6	21	24	584.91	0.46	−0.64	*Berthelina* sp.	2
1050	29	6	21	24	584.91	0.257	−0.464	*Berthelina* sp.	2
1050	29	5	72	75	583.92	1.701	−0.229	*Epistomina* sp.	2
1050	29	5	72	75	583.92	−0.199	−0.38	*Berthelina* sp.	2
1050	30	2	72	75	589.02	1.786	−0.38	*Epistomina* sp.	2
1050	30	3	72	75	590.52	1.777	−0.299	*Epistomina* sp.	2
1050	30	4	78	81	592.08	0.149	−0.509	*Berthelina intermedia*	2
1050	31	1	81	85	597.21	−0.009	−0.328	*Berthelina* sp.	2
1050	31	3	50	53	600.2	−0.065	−0.52	*Bethelina* sp.	2
1050	31	4	87	90	601.77	−0.948	−0.727	*Berthelina* sp.	2
1050	31	6	79	83	604.69	0.256	−0.66	*Berthelina* sp.	2
1050	31	CC			606	1.594	−1.54	*Berthelina* sp.	2
363	26	2	39	44	441.39	2.163	−0.846	*Gyroidinoides infracretacea*	1
363	27	1	38	41	458.88	2.393	−1.202	*Gyroidinoides infracretacea*	1
363	27	1	38	41	458.88	1.682	−0.934	*Gavelinella* sp.	1
363	28	1	38	41	478.28	1.865	−1.121	*Gavelinella* sp.	1
363	28	3	38	42	481.28	1.503	−0.536	*Gavelinella* sp.	1
511	49	4	43	46	427.93	0.451	−0.526	*Gyroidinoides infracretacea*	1
511	49	3	30	34	426.3	−0.518	0.078	*Gavelinella* sp.	1
511	49	4	43	46	427.93	1.237	−0.320	*Gavelinella* sp.	1
511	49	5	65.5	67.5	429.36	1.086	−0.558	*Berthelina* sp.	3
511	49	5	65.5	67.5	429.36	1.376	−0.448	*Berthelina* sp.	3
511	49	5	103	105	430.04	1.704	−0.555	*Berthelina* sp.	3
511	49	5	24	26	429.24	0.94	−0.38	*Gavelinella* sp.	2
511	49	6	24	26	430.74	1.38	−0.33	*G. globosa*	2
511	50	3	26	28	435.76	1.39	−0.24	*Gyroidinoides globosa*	2
511	49	5	61	63	429.61	1.61	−0.43	*Gavelinella* (plano-convex)	4
511	50	1	27	29	432.77	1.69	−0.36	*Gavelinella* (rounded)	4
511	50	1	27	29	432.77	1.66	−0.4	*Gavelinella* (rounded)	4
511	50	1	27	29	432.77	1.51	−0.47	*Gavelinella* (plano-convex)	4
511	50	2	53	55	434.53	1.44	−0.19	*Gavelinella* (plano-convex)	4
511	50	2	53	55	434.53	1.06	−0.66	*Gavelinella* (plano-convex)	4
511	50	2	53	55	434.53	1.22	−0.27	*Gavelinella* (plano-convex)	4
511	50	2	53	55	434.53	1.00	−0.35	*Gavelinella* (plano-convex)	4
511	50	3	52	54	436.02	1.80	−0.21	*Gavelinella* (plano-convex)	4
511	50	4	20	22	437.20	1.75	−0.12	*Gavelinella* (plano-convex)	4
511	50	CC	5	7	438.60	1.62	0.02	*Gavelinella* (plano-convex)	4
763B	23	1	40	43	389.9	−2.113	−0.237	*Gyroidinoides infracretacea*	1
763B	25	3	40	43	411.9	−0.414	−2.068	*Gyroidinoides infracretacea*	1
763B	28	3	40	43	440.4	0.486	−0.040	*Gyroidinoides infracretacea*	1
763B	23	1	40	43	389.9	−1.951	−0.159	*Gavelinella* sp.	1
763B	25	3	40	43	411.9	0.783	−0.439	*Gavelinella* sp.	1
763B	28	3	40	43	440.4	0.583	−1.679	*Gavelinella* sp.	1

[a]References are as follows: 1, this study; 2, *Huber et al.* [2002]; 3, *Bice et al.* [2003]; and 4, *Fassell and Bralower* [1999].

[10] The sites with a hiatus immediately overlying NC10 (Sites 370, 398, 545, 550) are the same ones that also host the poorly preserved foraminifera (Figure 3, images with asterisks). The implied link between the hiatus and diagenetic alteration of benthic foraminifera in the immediately underlying sediments gains support from the observation (at Sites 370, 398 and 545) that foraminiferal $\delta^{18}O$ values measured at these sites are similar to those of equilibrium calcite at the seafloor during the subsequent interval of nonsedimentation (dashed gray lines in Figure 4). This suggests that the relatively high $\delta^{18}O$ signatures of these extremely poorly preserved foraminifera (Figure 3, images with asterisks) are a product of substantial diagenetic alteration while exposed at or near the seafloor during the interval of nonsedimentation represented by the Upper Cretaceous hiatus. We can be confident that diagenetic alteration of these foraminifera was not dominated by late-stage recrystallization at greater burial depths because of the large isotopic offsets between measured $\delta^{18}O$ and that of equilibrium calcite grown at the present burial depth (shown

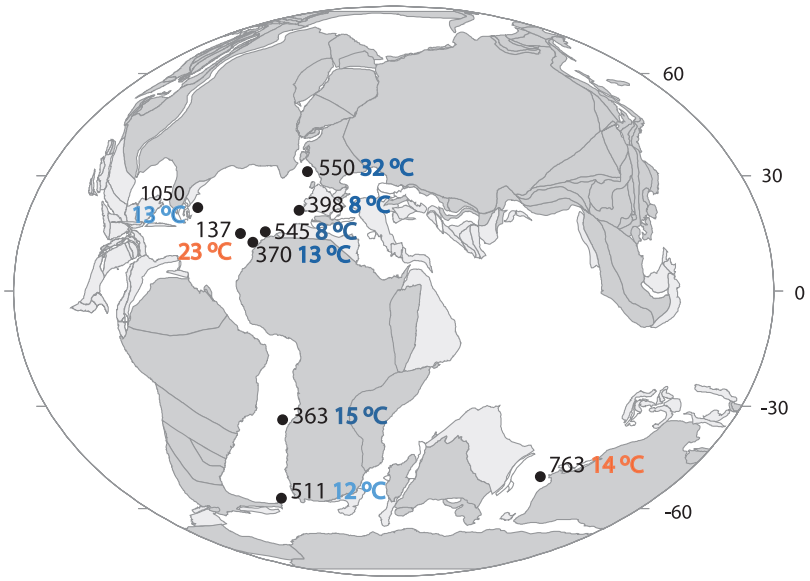

Figure 5. Paleogeographic reconstruction (as in Figure 1b) showing mean δ^{18}O-derived deep-ocean paleotemperatures for biozone NC10 at each site (based on δ^{18}O data in Figure 4). Numbers in colored font (colors as in Figures 2 and 4: dark blue, hiatus immediately overlying NC10; light blue, hiatus just above NC10; orange, no hiatus or its base is further up section) refer to paleotemperatures calculated using a $\delta^{18}O_w$ value of −1.0‰ (SMOW) (compatible with a deglaciated planet [*Shackleton and Kennett*, 1975]) and paleotemperature equation (1) of *Bemis et al.* [1998]. Note the generally much cooler δ^{18}O-derived paleotemperature estimates from North Atlantic sites with a hiatus immediately overlying NC10 (dark blue font).

by horizontal colored dashed lines). Recrystallization of North Atlantic benthic foraminifera at cooler BWTs during the Late Cretaceous is consistent with global compilations of foraminiferal δ^{18}O data indicating that, following the mid-Cretaceous acme of global warmth, ocean temperatures cooled globally by at least 7°C by the late Campanian [*Huber et al.*, 2002; *Shipboard Scientific Party*, 2002; *Wilson et al.*, 2002]. Cooler Late Cretaceous BWTs in the North Atlantic are also compatible with numerical modeling experiments predicting that Turonian BWTs in this basin cooled by 2 to 8°C from their Albian equivalents [*Poulsen et al.*, 2003], following the late Cenomanian [*Pletsch et al.*, 2001] connection to the wider, global ocean. Instead of recrystallization at the seafloor, the exceptionally low foraminiferal δ^{18}O values from Site 550 suggest late-stage recrystallization at substantial burial depths (e.g., about 400 m (Figure 4)) under the influence of high "geothermal" temperatures and low pore fluid δ^{18}O.

[11] In Figure 5 we show calculated BWTs for each site based on the NC10 benthic foraminifer δ^{18}O data from Figure 4 (colors as in Figure 4). In line with their relatively high measured δ^{18}O values, diagenetically altered benthic foraminifera from North Atlantic sites with a hiatus immediately overlying NC10 (Sites 370, 398, 545) yield anomalously cool estimates of deep-ocean temperature (dark blue numbers in Figure 5). It is notable that Site 370 provides somewhat warmer paleotemperatures, in line with its apparently less severe diagenetic alteration (Figure 3), probably a consequence of its clay-rich lithology (Figure 2). The anomalously cool latest Albian/earliest Cenomanian paleotemperatures (dark blue numbers in Figure 5) are inconsistent both with our contemporaneous warmer deep-ocean paleotemperatures from sites with much better preserved benthic foraminifera (orange numbers in Figure 5) and with predictions of extreme deep-ocean warmth in the Albian North Atlantic from numerical modeling [*Poulsen et al.*, 2001]. The site in the North Atlantic (1050) with a hiatus just above NC10 yields intermediate temperatures (light blue number) similar to those from Site 370. However, the equivalent site (i.e., light blue) outside the North Atlantic (Site 511) registers temperatures that are in line with those from another high-latitude Southern Hemisphere site hosting well-preserved foraminifera (e.g., 763B). Despite the presence of a hiatus at Site 511 just above NC10 (Figure 2), it appears that its clay-rich lithology (Figure 2) inhibited diagenetic alteration (Figure 3).

6. Upper Cretaceous Hiatus and Equatorial Atlantic Gateway Opening

[12] If our interpretation of the δ^{18}O data is correct then we can constrain the timing of the alteration of the poorly preserved foraminifera to fall between the age of the altered foraminifera (earliest possible date) and the top of the hiatus (i.e., sometime between the earliest Cenomanian, ~99 Ma ago, and the Coniacian to middle Campanian, 86 to 77 Ma ago). This age range for alteration is compatible with independent estimates of the timing of equatorial Atlantic gateway opening [*Pletsch et al.*, 2001; *Friedrich and Erbacher*, 2006].

[13] Our findings suggest that the extensive Upper Cretaceous hiatus documented in the North Atlantic Ocean was perhaps somehow linked to the opening of the equatorial Atlantic gateway. Following gateway opening between Cenomanian [*Pletsch et al.*, 2001] and Campanian [*Friedrich and Erbacher*, 2006] time, deep waters of the North Atlantic finally became fully connected with the cooler global ocean. As a consequence, foraminifera of NC10 age at shallow burial depths or exposed at the seafloor came into contact with much cooler, and potentially more corrosive, deep waters than those in which they had lived. Under typical pelagic sedimentary conditions, interstitial pore waters are buffered with respect to carbonate ion concentrations ($[CO_3^{2-}]$) owing to the dissolution of biogenic carbonates. However, this was not the case for the poorly preserved North Atlantic foraminifera documented in this study because of the prolonged sedimentary hiatus (although clay-rich lithologies appear to have somewhat reduced the diaganetic impact of the hiatus).

[14] The cause of the widespread hiatus was likely either strengthened vigor in bottom water currents (i.e., physical erosion) or more corrosive deep waters (i.e., chemical dissolution) within the newly opened North Atlantic. Evidence in support of dissolution is found in the stratigraphic record of $CaCO_3$ content of North Atlantic sediments through the Upper Cretaceous. Where Cenomanian to Campanian sediments are found in the North Atlantic they are typically red or multicolored clay with extremely low ($\leq$ a few %) $CaCO_3$ contents (at paleodepths from 5.5 up to at least 2.5 km) [*Thierstein*, 1979; *Tucholke and Vogt*, 1979; *Arthur and Dean*, 1986] and accumulated at extremely low sedimentation rates (<1 m/Ma). This prominence of clay in the North Atlantic persists from the lower Cenomanian ($\sim$99 Ma ago) to the upper Campanian ($\sim$75 Ma ago), a stratigraphic interval corresponding closely to that of the extensive sedimentary hiatus (Figure 2). This preponderance of clay (and absence of $CaCO_3$) suggests a prolonged ($\sim$24 Ma) interval of comparatively shallow ($\leq$2.5 km [*Tucholke and Vogt*, 1979; *Arthur and Dean*, 1986]) calcite compensation depths (CCDs). This shallow CCD state is presumably, at least in part, attributable to high eustatic sea levels during the Late Cretaceous [*Haq et al.*, 1987], submerging continental shelves and, through widespread shelf deposition of calcareous microfossils [*Roth*, 1986], causing enhanced basin to shelf fractionation of $CaCO_3$ [*Hays and Pitman*, 1973; *Berger and Winterer*, 1974; *Sclater et al.*, 1979; *Opdyke and Wilkinson*, 1988]. Yet, this sedimentation regime has also been tentatively linked to the opening of the equatorial Atlantic gateway [*Poulsen et al.*, 2003], presumably through incursion of more corrosive deep waters into the previously isolated North Atlantic basin. Our results, and our documentation of a temporal coincidence between the duration of the hiatus, a $CaCO_3$-poor sedimentation regime and estimates of gateway opening, lend support to this view.

7. Conclusions

[15] Diagenetic alteration of planktic foraminiferal calcite from tropical latitudes at the seafloor is now the widely accepted mechanism to explain a long-standing discrepancy during past "greenhouse" climates between relatively cool foraminiferal $\delta^{18}O$-derived tropical SSTs in comparison to much warmer tropical temperatures predicted by numerical models [*Schrag et al.*, 1995; *Wilson and Opdyke*, 1996; *Norris and Wilson*, 1998; *Pearson et al.*, 2001; *Wilson et al.*, 2002; *Sexton et al.*, 2006a]. In contrast, the taphonomy of benthic foraminiferal calcite, and its influence on the deep-sea paleotemperature record, has received little attention. Numerical modeling indicates that the carbonate recrystallization histories of deep-sea sections are dominated by events in their early burial history [*Rudnicki et al.*, 2001]. This means that the effect of benthic foraminiferal diagenetic alteration on the deep-sea paleotemperature record should be strongly influenced by the extent of postburial sediment–pore fluid exchange. The rate of this exchange will likely be determined by sedimentation rate and lithology. We show that an extreme change in sedimentation rate (a prolonged and widespread Upper Cretaceous sedimentary hiatus in the North Atlantic) had a major, detrimental impact on the taphonomy and $\delta^{18}O$ of benthic foraminiferal calcite from underlying mid-Cretaceous (nannofossil biozone NC10, $\sim$99 Ma ago) strata at multiple sites.

[16] Scanning electron microscopy of whole tests gives a false impression of the preservation state of benthic foraminifera. Whole tests appear to show at least moderate preservation at all sites whereas SEM images of cross sections of test walls reveal this to be a misleading picture. We find that, at sites where the hiatus immediately overlies sediments of NC10 age, benthic foraminifera are typically extremely poorly preserved internally, with $\delta^{18}O$ values substantially higher than those from contemporaneous better preserved benthic foraminifera at sites without an immediately overlying hiatus. These anomalously high $\delta^{18}O$ values are similar to estimated $\delta^{18}O$ values for calcite precipitated in equilibrium with cooler, Late Cretaceous deep waters during the subsequent interval of nonsedimentation. We interpret these observations to indicate that benthic foraminifera were heavily altered while exposed at (or very near) the seafloor for a prolonged period of time during the Late Cretaceous. Sediment lithology appears to modulate the intensity of alteration, with clay-rich sediments affording foraminifera most protection.

[17] Our results suggest that sedimentation rate and lithology together determine the extent of diagenetic alteration. The importance of these two variables is probably a function of their mutual influence on the degree of exchange between sediments and pore fluids. Sedimentation rates control sediment–pore fluid exchange via diffusion (the effects of distance, gradients and flux), while lithology regulates exchange via porosity. Furthermore, our results point to the postdepositional alteration of individual foraminifera being a slower and longer-lived process than the maximal time span for alteration of $\sim$10 Ma suggested by numerical model analysis of bulk carbonate [*Rudnicki et al.*, 2001], with important paleoceanographic implications. Our findings also highlight the importance of detailed examination of the taphonomy of benthic foraminiferal wall structures in paleoceanographic studies.

[18] **Acknowledgments.** We thank Mike Bolshaw, Matt Cooper, and Richard Pearce for laboratory assistance and Oliver Friedrich, Agostino Merico, and Richard Norris for useful discussions. We also thank Mike Arthur and Brian Huber for constructive reviews and Gerald Dickens for valuable editorial suggestions. This research used samples and data provided by the Ocean Drilling Program (ODP). ODP (now IODP) is sponsored by the U.S. National Science Foundation and participating countries under the management of Joint Oceanographic Institutions, Inc. Financial support was provided by a Natural Environment Research Council (NERC) studentship (to P.F.S.), a European Commission Marie Curie Outgoing International Fellowship (to P.F.S.), and a NERC grant (to P.A.W.).

References

Arthur, M. A., and W. E. Dean (1986), Cretaceous paleoceanography, in *The Geology of North America*, vol. M, *The Western North Atlantic Region*, edited by B. E. Tucholke and P. R. Vogt, pp. 617–630, Geol. Soc. of Am., Boulder, Colo.

Barrera, E. (1994), Global environmental changes preceding the Cretaceous-Tertiary boundary: Early–late Maastrichtian transition, *Geology*, *22*, 877–880, doi:10.1130/0091-7613(1994)022<0877:GECPTC>2.3.CO;2.

Barrera, E., and B. T. Huber (1991), Paleogene and early Neogene oceanography of the southern Indian Ocean: Leg 119 foraminifer stable isotope results, *Proc. Ocean Drill. Program Sci. Results*, *119*, 693–717.

Barron, E. J., and W. M. Washington (1985), Warm Cretaceous climates: High atmospheric CO_2 as a plausible explanation, in *The Carbon Cycle and Atmospheric CO_2: Natural Variations Archaean to Present*, *Geophys. Monogr. Ser.*, vol. 32, edited by E. T. Sundquist and W. S. Broecker, pp. 546–553, AGU, Washington, D. C.

Bemis, B. E., H. J. Spero, J. Bijma, and D. W. Lea (1998), Reevaluation of the oxygen isotopic composition of planktonic foraminifera: Experimental results and revised paleotemperature equations, *Paleoceanography*, *13*, 150–160, doi:10.1029/98PA00070.

Berger, W. H., and E. L. Winterer (1974), Plate stratigraphy and the fluctuating carbonate line, in *Pelagic Sediments: On Land and Under the Sea*, edited by K. J. Hsü and H. C. Jenkyns, *Spec. Publ. Int. Assoc. Sedimentol.*, *1*, 11–48.

Berner, R. A., and Z. Kothavala (2001), GEOCARB III: A revised model of atmospheric CO_2 over Phanerozoic time, *Am. J. Sci.*, *301*, 182–204, doi:10.2475/ajs.301.2.182.

Berner, R. A., A. C. Lasaga, and R. M. Garrels (1983), The carbonate-silicate geochemical cycle and its effect on atmospheric carbon-dioxide over the past 100 million years, *Am. J. Sci.*, *283*, 641–683.

Bice, K. L., and R. D. Norris (2002), Possible atmospheric CO_2 extremes of the Middle Cretaceous (late Albian–Turonian), *Paleoceanography*, *17*(4), 1070, doi:10.1029/2002PA000778.

Bice, K. L., B. T. Huber, and R. D. Norris (2003), Extreme polar warmth during the Cretaceous greenhouse?: Paradox of the late Turonian $\delta^{18}O$ record at Deep Sea Drilling Project Site 511, *Paleoceanography*, *18*(2), 1031, doi:10.1029/2002PA000848.

Boersma, A., I. P. Silva, and N. J. Shackleton (1987), Atlantic Eocene planktonic foraminiferal paleohydrographic indicators and stable isotope paleoceanography, *Paleoceanography*, *2*, 287–331, doi:10.1029/PA002i003p00287.

Bralower, T. J., J. C. Zachos, E. Thomas, M. Parrow, C. K. Paull, D. C. Kelly, I. P. Silva, W. V. Sliter, and K. C. Lohmann (1995), Late Paleocene to Eocene paleoceanography of the equatorial Pacific Ocean: Stable isotopes recorded at Ocean Drilling Program Site 865, Allison Guyot, *Paleoceanography*, *10*, 841–865, doi:10.1029/95PA01143.

Bralower, T. J., P. D. Fullagar, C. K. Paull, G. S. Dwyer, and R. M. Leckie (1997), Mid-Cretaceous strontium-isotope stratigraphy of deep-sea sections, *Geol. Soc. Am. Bull.*, *109*, 1421–1422, doi:10.1130/0016-7606(1997)109<1421:MCSISO>2.3.CO;2.

Burnett, J. A. (1999), Upper Cretaceous, in *Calcareous Nannofossil Biostratigraphy*, edited by P. R. Bown, pp. 132–139, Chapman and Hall, London.

Bush, A. B. G., and S. G. H. Philander (1997), The Late Cretaceous: Simulation with a coupled atmosphere-ocean general circulation model, *Paleoceanography*, *12*, 495–516, doi:10.1029/97PA00721.

Carman, M. R., and L. D. Keigwin (2004), Preservation and color differences in *Nuttallides umbonifera*, *J. Foraminiferal Res.*, *34*, 102–108, doi:10.2113/0340102.

Corliss, B. H., and S. Honjo (1981), Dissolution of deep-sea benthonic foraminifera, *Micropaleontology*, *27*, 356–378, doi:10.2307/1485191.

Crowley, T. J. (1991), Past CO_2 changes and tropical sea surface temperatures, *Paleoceanography*, *6*, 387–394, doi:10.1029/91PA00432.

Crowley, T. J., and G. R. North (1991), *Paleoclimatology*, 339 pp., Oxford Univ. Press, New York.

Crowley, T. J., and J. C. Zachos (2000), Comparison of zonal temperature profiles for past warm time periods, in *Warm Climates in Earth History*, edited by B. Huber, K. MacLeod, and S. Wing, pp. 50–76, Cambridge Univ. Press, Cambridge, U. K.

D'Hondt, S., and M. A. Arthur (1996), Late Cretaceous oceans and the cool tropic paradox, *Science*, *271*, 1838–1841, doi:10.1126/science.271.5257.1838.

Douglas, R. G., and S. M. Savin (1973), Oxygen and carbon isotope analyses of Cretaceous and Tertiary foraminifera from the central North Pacific, *Initial Rep. Deep Sea Drill. Proj.*, *17*, 591–607.

Douglas, R. G., and S. M. Savin (1975), Oxygen and carbon isotope analyses of Tertiary and Cretaceous microfossils from Shatsky Rise and other sites in the North Pacific Ocean, *Initial Rep. Deep Sea Drill. Proj.*, *32*, 509–520.

Erba, E., I. Premoli Silva, and D. K. Watkins (1995), Cretaceous calcareous plankton biostratigraphy of Sites 872 through 879, *Proc. Ocean Drill. Program Sci. Results*, *144*, 157–169.

Fassell, M. L., and T. J. Bralower (1999), A warm, equable mid-Cretaceous: Stable isotope evidence, in *Evolution of the Cretaceous Ocean-Climate System*, edited by E. Barrera and C. C. Johnson, *Spec. Pap. Geol. Soc. Am.*, *332*, 121–142.

Friedrich, O., and J. Erbacher (2006), Benthic foraminiferal assemblages from Demerara Rise (ODP Leg 207, western tropical Atlantic): Possible evidence for a progressive opening of the equatorial Atlantic gateway, *Cretaceous Res.*, *27*, 377–397, doi:10.1016/j.cretres.2005.07.006.

Haq, B. U., J. Hardenbol, and P. R. Vail (1987), Chronology of fluctuating sea levels since the Triassic, *Science*, *235*, 1156–1167, doi:10.1126/science.235.4793.1156.

Hayes, D. E., A. C. Pimm, J. P. Beckmann, W. E. Benson, W. H. Berger, P. H. Roth, P. R. Supko, and U. von Rad (1972), Shipboard site reports: Site 137, *Initial Rep. Deep Sea Drill. Proj.*, *14*, 85–95, doi:10.2973/dsdp.proc.14.1972.

Hays, J. D., and W. C. I. Pitman (1973), Lithospheric plate motion, sea level changes and climatic and ecological consequences, *Nature*, *246*, 18–22, doi:10.1038/246018a0.

Huber, B. T., D. A. Hodell, and C. P. Hamilton (1995), Middle–Late Cretaceous climate of the southern high latitudes: Stable isotopic evidence for minimal equator-to-pole thermal gradients, *Geol. Soc. Am. Bull.*, *107*, 1164–1191.

Huber, B. T., R. D. Norris, and K. G. MacLeod (2002), Deep-sea paleotemperature record of extreme warmth during the Cretaceous, *Geology*, *30*, 123–126, doi:10.1130/0091-7613(2002)030<0123:DSPROE>2.0.CO;2.

Huber, M., and L. C. Sloan (2000), Climatic responses to tropical sea surface temperature changes on a "greenhouse" Earth, *Paleoceanography*, *15*, 443–450, doi:10.1029/1999PA000455.

Huber, M., and L. C. Sloan (2001), Heat transport, deep waters, and thermal gradients: Coupled simulation of an Eocene greenhouse climate, *Geophys. Res. Lett.*, *28*, 3481–3484, doi:10.1029/2001GL012943.

Larson, R. L. (1991), The latest pulse of Earth: Evidence for a mid-Cretaceous superplume, *Geology*, *19*, 547–550, doi:10.1130/0091-7613(1991)019<0547:LPOEEF>2.3.CO;2.

Lawrence, J. R., and J. M. Gieskes (1981), Constraints on water transport and alteration in the oceanic crust from the isotopic composition of pore water, *J. Geophys. Res.*, *86*, 7924–7934, doi:10.1029/JB086iB09p07924.

Manabe, S., and K. Bryan Jr. (1985), CO_2-induced change in a coupled ocean-atmosphere model and its paleoclimatic implications, *J. Geophys. Res.*, *90*, 11,689–11,707.

McCorkle, D. C., P. A. Martin, D. W. Lea, and G. P. Klinkhammer (1995), Evidence of a dissolution effect on benthic foraminiferal shell chemistry: $\delta^{13}C$, Cd/Ca, Ba/Ca, and Sr/Ca results from the Ontong Java Plateau, *Paleoceanography*, *10*, 699–714, doi:10.1029/95PA01427.

Moriya, K., P. A. Wilson, O. Friedrich, J. Erbacher, and H. Kawahata (2007), Testing for ice sheets during the mid-Cretaceous greenhouse using glassy foraminiferal calcite from the mid-Cenomanian tropics on Demerara Rise, *Geology*, *35*, 615–618, doi:10.1130/G23589A.1.

Murray, J. W. (1989), Syndepositional dissolution of calcareous foraminifera in modern shallow-water sediments, *Mar. Micropaleontol.*, *15*, 117–121, doi:10.1016/0377-8398(89)90007-8.

Norris, R. D., and P. A. Wilson (1998), Low-latitude sea-surface temperatures for the mid-Cretaceous and the evolution of planktic

foraminifera, *Geology*, *26*, 823–826, doi:10.1130/0091-7613(1998)026<0823:LLSSTF>2.3.CO;2.

Norris, R. D., K. L. Bice, E. A. Magno, and P. A. Wilson (2002), Jiggling the tropical thermostat in the Cretaceous hothouse, *Geology*, *30*, 299–302, doi:10.1130/0091-7613(2002)030<0299:JTTTIT>2.0.CO;2.

Opdyke, B. N., and B. H. Wilkinson (1988), Surface area control of shallow cratonic to deep marine carbonate accumulation, *Paleoceanography*, *3*, 685–703, doi:10.1029/PA003i006p00685.

Pearson, P. N., P. W. Ditchfield, J. Singano, K. G. Harcourt-Brown, C. J. Nicholas, R. K. Olsson, N. J. Shackleton, and M. A. Hall (2001), Warm tropical sea surface temperatures in the Late Cretaceous and Eocene epochs, *Nature*, *413*, 481–487, doi:10.1038/35097000.

Pearson, P. N., B. E. van Dongen, C. J. Nicholas, R. D. Pancost, S. Schouten, J. M. Singano, and B. S. Wade (2007), Stable warm tropical climate through the Eocene epoch, *Geology*, *35*, 211–214, doi:10.1130/G23175A.1.

Pletsch, T., J. Erbacher, A. E. L. Holbourn, W. Kuhnt, M. Moullade, F. E. Oboh-Ikuenobede, E. Soding, and T. Wagner (2001), Cretaceous separation of Africa and South America: The view from the West African margin (ODP Leg 159), *J. South Am. Earth Sci.*, *14*, 147–174, doi:10.1016/S0895-9811(01)00020-7.

Poulsen, C. J., E. J. Barron, M. A. Arthur, and W. H. Peterson (2001), Response of the mid-Cretaceous global oceanic circulation to tectonic and CO_2 forcings, *Paleoceanography*, *16*, 576–592, doi:10.1029/2000PA000579.

Poulsen, C. J., A. S. Gendaszek, and R. L. Jacob (2003), Did the rifting of the Atlantic Ocean cause the Cretaceous thermal maximum?, *Geology*, *31*, 115–118, doi:10.1130/0091-7613(2003)031<0115:DTROTA>2.0.CO;2.

Premoli Silva, I., and W. V. Sliter (1999), Cretaceous paleoceanography: Evidence from planktonic foraminiferal evolution, in *Evolution of the Cretaceous Ocean-Climate System*, edited by E. Barrera and C. C. Johnson, *Spec. Pap. Geol. Soc. Am.*, *332*, 301–328.

Price, G. D., B. W. Sellwood, R. M. Corfield, L. Clarke, and J. E. Cartlidge (1998), Isotopic evidence for palaeotemperatures and depth stratification of Middle Cretaceous planktonic foraminifera from the Pacific Ocean, *Geol. Mag.*, *135*, 183–191, doi:10.1017/S0016756898008334.

Rao, Y. H., C. Subrahmanyam, S. R. Sharma, A. A. Rastogi, and B. Deka (2001), Estimates of geothermal gradients and heat flow from BSRs along the western continental margin of India, *Geophys. Res. Lett.*, *28*, 355–358, doi:10.1029/2000GL008528.

Roth, P. H. (1986), Mesozoic palaeoceanography of the North Atlantic and Tethys oceans, in *North Atlantic Palaeoceanography*, edited by C. P. Summerhayes and N. J. Shackleton, *Geol. Soc. Spec. Publ.*, *21*, 299–320.

Rudnicki, M. D., P. A. Wilson, and W. T. Anderson (2001), Numerical models of diagenesis, sediment properties, and pore fluid chemistry on a paleoceanographic transect: Blake Nose, Ocean Drilling Program Leg 171B, *Paleoceanography*, *16*, 563–575, doi:10.1029/2000PA000551.

Savin, S. M. (1977), The history of the Earth's surface temperature during the past 100 million years, *Annu. Rev. Earth Planet. Sci.*, *5*, 319–355, doi:10.1146/annurev.ea.05.050177.001535.

Schlanger, S. O., H. C. Jenkyns, and I. Premoli-Silva (1981), Volcanism and vertical tectonics in the Pacific Basin related to global Cretaceous transgressions, *Earth Planet. Sci. Lett.*, *52*, 435–449, doi:10.1016/0012-821X(81)90196-5.

Schrag, D. P., D. J. DePaolo, and F. M. Richter (1995), Reconstructing past sea surface temperatures: Correcting for diagenesis of bulk marine carbonate, *Geochim. Cosmochim. Acta*, *59*, 2265–2278, doi:10.1016/0016-7037(95)00105-9.

Sclater, J. G., E. Boyle, and J. M. Edmond (1979), A quantitative analysis of some factors affecting carbonate sedimentation in the oceans, in *Deep Drilling Results in the Atlantic Ocean: Continental Margins and Paleoenvironment*, *Maurice Ewing Ser.*, vol. 3, edited by M. Talwani, W. Hay, and W. B. F. Ryan, pp. 235–248, AGU, Washington, D. C.

Sexton, P. F., P. A. Wilson, and P. N. Pearson (2006a), Microstructural and geochemical perspectives on planktic foraminiferal preservation: "Glassy" versus "frosty", *Geochem. Geophys. Geosyst.*, *7*, Q12P19, doi:10.1029/2006GC001291.

Sexton, P. F., P. A. Wilson, and P. N. Pearson (2006b), Palaeoecology of late middle Eocene planktic foraminifera and evolutionary implications, *Mar. Micropaleontol.*, *60*, 1–16, doi:10.1016/j.marmicro.2006.02.006.

Shackleton, N., and A. Boersma (1981), The climate of the Eocene ocean, *J. Geol. Soc. London*, *138*, 153–157, doi:10.1144/gsjgs.138.2.0153.

Shackleton, N. J., and J. P. Kennett (1975), Paleotemperature history of the Cenozoic and the initiation of Antarctic glaciation: Oxygen and carbon isotope analysis in DSDP sites 277, 279 and 281, *Initial Rep. Deep Sea Drill. Proj.*, *29*, 743–756.

Shipboard Scientific Party (1978), Walvis Ridge—Sites 362 and 363, *Initial Rep. Deep Sea Drill. Proj.*, *40*, 183–356.

Shipboard Scientific Party (1979), Site 398, *Initial Rep. Deep Sea Drill. Proj.*, *47*, 761–775.

Shipboard Scientific Party (1983), Site 511, *Initial Rep. Deep Sea Drill. Proj.*, *71*, 21–109.

Shipboard Scientific Party (1984), Site 545, *Initial Rep. Deep Sea Drill. Proj.*, *79*, 81–177.

Shipboard Scientific Party (1985), Site 550, *Initial Rep. Deep Sea Drill. Proj.*, *80*, 251–355.

Shipboard Scientific Party (1990), Site 763, *Proc. Ocean Drill. Program Initial Rep.*, *122*, 289–352.

Shipboard Scientific Party (1998), Site 1050, *Proc. Ocean Drill. Program Initial Rep.*, *171B*, 93–169.

Shipboard Scientific Party (2002), Leg 198 summary, *Proc. Ocean Drill. Program Initial Rep.*, *198*, 1–148.

Shipboard Scientific Party (2004), Explanatory notes, *Proc. Ocean Drill. Program Initial Rep.*, *207*, 1–94.

Shipboard Scientific Party, and D. Bukry (1978), Site 370: Deep basin off Morocco, *Initial Rep. Deep Sea Drill. Proj.*, *41*, 421–491.

Sloan, L. C., and D. K. Rea (1996), Atmospheric carbon dioxide and early Eocene climate: A general circulation modeling sensitivity study, *Palaeogeogr. Palaeoclimatol. Palaeoecol.*, *119*, 275–292, doi:10.1016/0031-0182(95)00012-7.

Stott, L. D., J. P. Kennett, N. J. Shackleton, and R. M. Corfield (1990), The evolution of Antarctic surface waters during the Paleogene: Inferences from the stable isotopic composition of planktonic foraminifers, ODP Leg 113, *Proc. Ocean Drill. Program Sci. Results*, *113*, 849–863.

Thierstein, H. R. (1979), Paleoceanographic implications of organic carbon and carbonate distribution in Mesozoic deep sea sediments, in *Deep Drilling Results in the Atlantic Ocean: Continental Margins and Paleoenvironment*, edited by M. Talwani, W. Hay, and W. B. F. Ryan, pp. 249–274, AGU, Washington, D. C.

Tucholke, B. E., and P. R. Vogt (1979), Western North Atlantic: Sedimentary evolution and aspects of tectonic history, *Initial Rep. Deep Sea Drill. Proj.*, *43*, 791–825.

Veizer, J., Y. Godderis, and L. M. Francois (2000), Evidence for decoupling of atmospheric CO_2 and global climate during the Phanerozoic eon, *Nature*, *408*, 698–701, doi:10.1038/35047044.

Watkins, D. K., M. J. Cooper, and P. A. Wilson (2005), Calcareous nannoplankton response to late Albian oceanic anoxic event 1d in the western North Atlantic, *Paleoceanography*, *20*, PA2010, doi:10.1029/2004PA001097.

Widmark, J. G. V., and B. A. Malmgren (1988), Differential dissolution of Upper Cretaceous deep-sea benthonic foraminifers from the Angola Basin, South Atlantic Ocean, *Mar. Micropaleontol.*, *13*, 47–78, doi:10.1016/0377-8398(88)90012-6.

Wilson, P. A., and R. D. Norris (2001), Warm tropical ocean surface and global anoxia during the mid-Cretaceous period, *Nature*, *412*, 425–429, doi:10.1038/35086553.

Wilson, P. A., and B. N. Opdyke (1996), Equatorial sea-surface temperatures for the Maastrichtian revealed through remarkable preservation of metastable carbonate, *Geology*, *24*, 555–558, doi:10.1130/0091-7613(1996)024<0555:ESSTFT>2.3.CO;2.

Wilson, P. A., R. D. Norris, and M. J. Cooper (2002), Testing the Cretaceous greenhouse hypothesis using glassy foraminiferal calcite from the core of the Turonian tropics on Demerara Rise, *Geology*, *30*, 607–610, doi:10.1130/0091-7613(2002)030<0607:TTCGHU>2.0.CO;2.

Zachos, J. C., L. D. Stott, and K. C. Lohmann (1994), Evolution of Early Cenozoic marine temperatures, *Paleoceanography*, *9*, 353–387, doi:10.1029/93PA03266.

Zachos, J. C., M. A. Arthur, T. J. Bralower, and H. J. Spero (2002), Palaeoclimatology (communication arising): Tropical temperatures in greenhouse episodes, *Nature*, *419*, 897–898, doi:10.1038/419897b.

P. F. Sexton, School of Earth and Ocean Sciences, Cardiff University, Cardiff CF10 3YE, UK. (sextonpf@cardiff.ac.uk)

P. A. Wilson, National Oceanography Centre, University of Southampton, European Way, Southampton SO14 3ZH, UK.